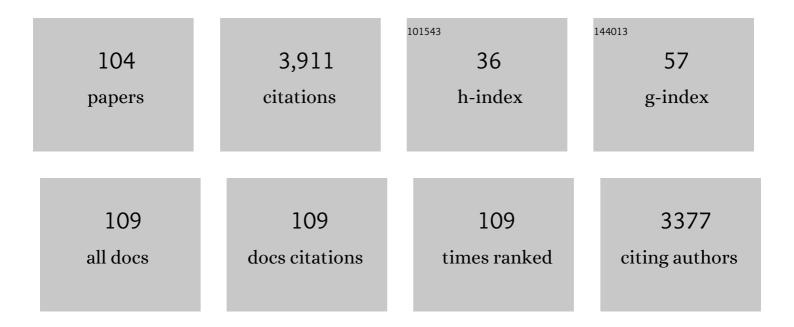
Dirk Klaeschen

List of Publications by Year in descending order

Source: https://exaly.com/author-pdf/6240377/publications.pdf Version: 2024-02-01



#	Article	IF	CITATIONS
1	Insights Into Exhumation and Mantle Hydration Processes at the Deep Galicia Margin From a 3D Highâ€Resolution Seismic Velocity Model. Journal of Geophysical Research: Solid Earth, 2022, 127, .	3.4	1
2	Megathrust reflectivity reveals the updip limit of the 2014 Iquique earthquake rupture. Nature Communications, 2022, 13, .	12.8	4
3	Subducting oceanic basement roughness impacts on upper-plate tectonic structure and a backstop splay fault zone activated in the southern Kodiak aftershock region of the Mw 9.2, 1964 megathrust rupture, Alaska. , 2021, 17, 409-437.		5
4	Comparison of 2-D and 3-D full waveform inversion imaging using wide-angle seismic data from the Deep Galicia Margin. Geophysical Journal International, 2021, 227, 228-256.	2.4	3
5	Relationship Between Subduction Erosion and the Upâ€Dip Limit of the 2014 Mw 8.1 Iquique Earthquake. Geophysical Research Letters, 2021, 48, e2020GL092207.	4.0	10
6	Marine forearc structure of eastern Java and its role in the 1994 Java tsunami earthquake. Solid Earth, 2021, 12, 2467-2477.	2.8	5
7	New insights into geology and geochemistry of the Kerch seep area in the Black Sea. Marine and Petroleum Geology, 2020, 113, 104162.	3.3	13
8	Subducted sediments, upper-plate deformation and dewatering at New Zealand's southern Hikurangi subduction margin. Earth and Planetary Science Letters, 2020, 530, 115945.	4.4	15
9	Detachment tectonics at Mid-Atlantic Ridge 26°N. Scientific Reports, 2019, 9, 11830.	3.3	12
10	From gradual spreading to catastrophic collapse – Reconstruction of the 1888 Ritter Island volcanic sector collapse from high-resolution 3D seismic data. Earth and Planetary Science Letters, 2019, 517, 1-13.	4.4	44
11	Ionian Abyssal Plain: a window into the Tethys oceanic lithosphere. Solid Earth, 2019, 10, 447-462.	2.8	19
12	Tectonic Controls on Gas Hydrate Distribution Off SW Taiwan. Journal of Geophysical Research: Solid Earth, 2019, 124, 1164-1184.	3.4	30
13	Resolving the fine-scale velocity structure of continental hyperextension at the Deep Galicia Margin using full-waveform inversion. Geophysical Journal International, 2018, 212, 244-263.	2.4	23
14	Elongate fluid flow structures: Stress control on gas migration at Opouawe Bank, New Zealand. Marine and Petroleum Geology, 2018, 92, 913-931.	3.3	9
15	Morphostructure, tectonoâ€sedimentary evolution and seismic potential of the Horseshoe Fault, <scp>SW</scp> Iberian Margin. Basin Research, 2018, 30, 382-400.	2.7	18
16	Deep structure of the Porcupine Basin from wide-angle seismic data. Petroleum Geology Conference Proceedings, 2018, 8, 199-209.	0.7	19
17	From Continental Hyperextension to Seafloor Spreading: New Insights on the Porcupine Basin From Wideâ€Angle Seismic Data. Journal of Geophysical Research: Solid Earth, 2018, 123, 8312-8330.	3.4	16
18	A first estimation of gas hydrates offshore Patagonia (Chile). Marine and Petroleum Geology, 2018, 96, 232-239.	3.3	15

#	Article	IF	CITATIONS
19	On the origin of multiple BSRs in the Danube deep-sea fan, Black Sea. Earth and Planetary Science Letters, 2017, 462, 15-25.	4.4	59
20	Crustal strain-dependent serpentinisation in the Porcupine Basin, offshore Ireland. Earth and Planetary Science Letters, 2017, 474, 148-159.	4.4	32
21	Dual-vergence structure from multiple migration of widely spaced OBSs. Tectonophysics, 2017, 718, 45-60.	2.2	7
22	Seismic Oceanography in the Tyrrhenian Sea: Thermohaline Staircases, Eddies, and Internal Waves. Journal of Geophysical Research: Oceans, 2017, 122, 8503-8523.	2.6	22
23	Gas hydrate distribution and hydrocarbon maturation north of the Knipovich Ridge, western Svalbard margin. Journal of Geophysical Research: Solid Earth, 2016, 121, 1405-1424.	3.4	26
24	Splay fault branching from the <scp>H</scp> ikurangi subduction shear zone: Implications for slow slip and fluid flow. Geochemistry, Geophysics, Geosystems, 2016, 17, 5009-5023.	2.5	23
25	Continental hyperextension, mantle exhumation, and thin oceanic crust at the continentâ€ocean transition, West Iberia: New insights from wideâ€angle seismic. Journal of Geophysical Research: Solid Earth, 2016, 121, 3177-3199.	3.4	53
26	A Possible Source Mechanism of the 1946 Unimak Alaska Far-Field Tsunami: Uplift of the Mid-Slope Terrace Above a Splay Fault Zone. Pure and Applied Geophysics, 2016, 173, 4189-4201.	1.9	11
27	Characterization of the submesoscale energy cascade in the Alboran Sea thermocline from spectral analysis of highâ€resolution MCS data. Geophysical Research Letters, 2016, 43, 6461-6468.	4.0	22
28	The Ionian and Alfeo–Etna fault zones: New segments of an evolving plate boundary in the central Mediterranean Sea?. Tectonophysics, 2016, 675, 69-90.	2.2	93
29	Gas migration through Opouawe Bank at the Hikurangi margin offshore New Zealand. Geo-Marine Letters, 2016, 36, 187-196.	1.1	18
30	Fault-controlled hydration of the upper mantle during continentalÂrifting. Nature Geoscience, 2016, 9, 384-388.	12.9	75
31	Seismic reflection imaging of mixing processes in Fram Strait. Journal of Geophysical Research: Oceans, 2015, 120, 6884-6896.	2.6	11
32	Gas-controlled seafloor doming. Geology, 2015, 43, 571-574.	4.4	56
33	Heat flow in the southern Chile forearc controlled by large-scale tectonic processes. Geo-Marine Letters, 2014, 34, 185-198.	1.1	21
34	The impact of fluid advection on gas hydrate stability: Investigations at sites of methane seepage offshore Costa Rica. Earth and Planetary Science Letters, 2014, 401, 95-109.	4.4	42
35	Submarine gas seepage in a mixed contractional and shear deformation regime: Cases from the Hikurangi obliqueâ€subduction margin. Geochemistry, Geophysics, Geosystems, 2014, 15, 416-433.	2.5	33
36	Crustal thinning in the northern Tyrrhenian Rift: Insights from multichannel and wideâ€angle seismic data across the basin. Journal of Geophysical Research: Solid Earth, 2014, 119, 1655-1677.	3.4	19

#	Article	IF	CITATIONS
37	<i>P</i> and <i>S</i> wave velocity measurements of water-rich sediments from the Nankai Trough, Japan. Journal of Geophysical Research: Solid Earth, 2014, 119, 787-805.	3.4	23
38	Insights into the emplacement dynamics of volcanic landslides from high-resolution 3D seismic data acquired offshore Montserrat, Lesser Antilles. Marine Geology, 2013, 335, 1-15.	2.1	39
39	Propagation of a lithospheric tear fault (STEP) through the western boundary of the Calabrian accretionary wedge offshore eastern Sicily (Southern Italy). Tectonophysics, 2013, 602, 141-152.	2.2	74
40	Subduction system variability across the segment boundary of the 2004/2005 Sumatra megathrust earthquakes. Earth and Planetary Science Letters, 2013, 365, 108-119.	4.4	16
41	Earlyâ€stage rifting of the northern Tyrrhenian Sea Basin: Results from a combined wideâ€angle and multichannel seismic study. Geochemistry, Geophysics, Geosystems, 2013, 14, 3032-3052.	2.5	41
42	Drivers of focused fluid flow and methane seepage at south Hydrate Ridge, offshore Oregon, USA. Geology, 2013, 41, 551-554.	4.4	35
43	Active deformation in old oceanic lithosphere and significance for earthquake hazard: Seismic imaging of the Coral Patch Ridge area and neighboring abyssal plains (SW Iberian Margin). Geochemistry, Geophysics, Geosystems, 2013, 14, 2206-2231.	2.5	42
44	Characterization of thermohaline staircases in the Tyrrhenian Sea using stochastic heterogeneity mapping. Proceedings of Meetings on Acoustics, 2013, , .	0.3	0
45	Evidence for active strike-slip faulting along the Eurasia-Africa convergence zone: Implications for seismic hazard in the southwest Iberian margin. Geology, 2012, 40, 495-498.	4.4	43
46	Seismic evidence for shallow gasâ€escape features associated with a retreating gas hydrate zone offshore west Svalbard. Journal of Geophysical Research, 2012, 117, .	3.3	47
47	Evolution of fluid expulsion and concentrated hydrate zones across the southern Hikurangi subduction margin, New Zealand: An analysis from depth migrated seismic data. Geochemistry, Geophysics, Geosystems, 2012, 13, .	2.5	74
48	Two-stage growth of the Calabrian accretionary wedge in the Ionian Sea (Central Mediterranean): Constraints from depthâ€migrated multichannel seismic data. Marine Geology, 2012, 326-328, 28-45.	2.1	32
49	Linked halokinesis and mud volcanism at the Mercator mud volcano, Gulf of Cadiz. Journal of Geophysical Research, 2011, 116, .	3.3	21
50	The Calabrian Arc subduction complex in the Ionian Sea: Regional architecture, active deformation, and seismic hazard. Tectonics, 2011, 30, .	2.8	159
51	Insights into active deformation in the Gulf of Cadiz from new 3-D seismic and high-resolution bathymetry data. Geochemistry, Geophysics, Geosystems, 2011, 12, n/a-n/a.	2.5	18
52	A Miocene tectonic inversion in the Ionian Sea (central Mediterranean): Evidence from multichannel seismic data. Journal of Geophysical Research, 2011, 116, .	3.3	48
53	Deep structure of the central Lesser Antilles Island Arc: Relevance for the formation of continental crust. Earth and Planetary Science Letters, 2011, 304, 121-134.	4.4	83
54	Margin architecture and seismic attenuation in the central Costa Rican forearc. Marine Geology, 2010, 276, 30-41.	2.1	5

#	Article	IF	CITATIONS
55	Stochastic Heterogeneity Mapping around a Mediterranean salt lens. Ocean Science, 2010, 6, 423-429.	3.4	9
56	Ocean temperature and salinity inverted from combined hydrographic and seismic data. Geophysical Research Letters, 2010, 37, .	4.0	65
57	High-resolution P-Cable 3D seismic imaging of gas chimney structures in gas hydrated sediments of an Arctic sediment drift. Marine and Petroleum Geology, 2010, 27, 1981-1994.	3.3	138
58	Crustal structure of the central Costa Rica subduction zone: implications for basal erosion from seismic wide-angle data. Geophysical Journal International, 2009, 178, 1112-1131.	2.4	17
59	Seismic reflection along the path of the Mediterranean Undercurrent. Continental Shelf Research, 2009, 29, 1848-1860.	1.8	31
60	Anatomy of the western Java plate interface from depth-migrated seismic images. Earth and Planetary Science Letters, 2009, 288, 399-407.	4.4	30
61	Estimating movement of reflectors in the water column using seismic oceanography. Geophysical Research Letters, 2009, 36, .	4.0	30
62	Estimating internal wave spectra using constrained models of the dynamic ocean. Geophysical Research Letters, 2009, 36, .	4.0	19
63	Effect of bandwidth on seismic imaging of rotating stratified turbulence surrounding an anticyclonic eddy from field data and numerical simulations. Geophysical Research Letters, 2009, 36, .	4.0	17
64	Effect of seismic source bandwidth on reflection sections to image water structure. Geophysical Research Letters, 2009, 36, .	4.0	26
65	High resolution seismic imaging of the ocean structure using a small volume airgun source array in the Gulf of Cadiz. Geophysical Research Letters, 2009, 36, .	4.0	17
66	Lower slope morphology of the Sumatra trench system. Basin Research, 2008, 20, 519-529.	2.7	37
67	Midâ€depth internal wave energy off the Iberian Peninsula estimated from seismic reflection data. Journal of Geophysical Research, 2008, 113, .	3.3	49
68	Heterogeneous deformation in the Cascadia convergent margin and its relation to thermal gradient (Washington, NW USA). Tectonics, 2008, 27, .	2.8	37
69	Potential of 3â€Ð vertical seismic profiles to characterize seismogenic fault zones. Geochemistry, Geophysics, Geosystems, 2008, 9, .	2.5	2
70	Tectonic framework of the mud mounds, associated BSRs and submarine landslides, offshore Nicaragua Pacific margin. Journal of the Geological Society, 2008, 165, 167-176.	2.1	6
71	Local seismic quantification of gas hydrates and BSR characterization from multi-frequency OBS data at northern Hydrate Ridge. Earth and Planetary Science Letters, 2007, 255, 414-431.	4.4	32
72	Movement along a low-angle normal fault: The S reflector west of Spain. Geochemistry, Geophysics, Geosystems, 2007, 8, n/a-n/a.	2.5	49

#	Article	IF	CITATIONS
73	High-resolution, deep tow, multichannel seismic and sidescan sonar survey of the submarine mounds and associated BSR off Nicaragua pacific margin. Marine Geology, 2007, 241, 33-43.	2.1	28
74	AVA analysis reveals in situ sediment diagenesis at the Costa Rican décollement. Sedimentary Geology, 2007, 196, 269-277.	2.1	2
75	Extreme crustal thinning in the south Porcupine Basin and the nature of the Porcupine Median High: implications for the formation of non-volcanic rifted margins. Journal of the Geological Society, 2004, 161, 783-798.	2.1	57
76	Seismic investigations of the O'Higgins Seamount Group and Juan Fernández Ridge: Aseismic ridge emplacement and lithosphere hydration. Tectonics, 2004, 23, n/a-n/a.	2.8	79
77	Upward delamination of Cascadia Basin sediment infill with landward frontal accretion thrusting caused by rapid glacial age material flux. Tectonics, 2004, 23, n/a-n/a.	2.8	67
78	The Mediterranean Ridge: A mass balance across the fastest growing accretionary complex on Earth. Journal of Geophysical Research, 2003, 108, .	3.3	58
79	Crustal structure of the Java margin from seismic wide-angle and multichannel reflection data. Journal of Geophysical Research, 2002, 107, ETG 1-1.	3.3	67
80	Frontal accretion along the western Mediterranean Ridge: the effect of Messinian evaporites on wedge mechanics and structural style. Marine Geology, 2002, 186, 59-82.	2.1	42
81	Extreme efficiency of mud volcanism in dewatering accretionary prisms. Earth and Planetary Science Letters, 2001, 189, 295-313.	4.4	90
82	Non-Coulomb wedges, wrong-way thrusting, and natural hazards in Cascadia. Geology, 2001, 29, 379.	4.4	63
83	Crustal structure of the central Sunda margin at the onset of oblique subduction. Geophysical Journal International, 2001, 147, 449-474.	2.4	88
84	Geophysical evidence for late stage magmatism at the central Ninetyeast Ridge, Eastern Indian Ocean. Marine Geophysical Researches, 2001, 22, 225-234.	1.2	8
85	Internal configuration of the Levantine Basin from seismic reflection data (eastern Mediterranean). Earth and Planetary Science Letters, 2000, 180, 77-89.	4.4	49
86	The continental margin off Oregon from seismic investigations. Tectonophysics, 2000, 329, 79-97.	2.2	49
87	Seismic images at the convergence zone from south of Cyprus to the Syrian coast, eastern Mediterranean. Tectonophysics, 2000, 329, 157-170.	2.2	36
88	Structure of the Makran subduction zone from wide-angle and reflection seismic data. Tectonophysics, 2000, 329, 171-191.	2.2	212
89	The structure of the Africa-Anatolia plate boundary in the eastern Mediterranean. Tectonics, 2000, 19, 723-739.	2.8	34
90	Relation between the Subducting Plate and Seismicity Associated with the Great 1964 Alaska Earthquake. Pure and Applied Geophysics, 1999, 154, 575-591.	1.9	23

#	Article	IF	CITATIONS
91	AVA analysis in the eastern Mediterranean. Physics and Chemistry of the Earth, 1999, 24, 467-474.	0.6	4
92	Opposing gradients of permanent strain in the aseismic zone and elastic strain across the seismogenic zone of the Kodiak shelf and slope, Alaska. Tectonics, 1999, 18, 248-262.	2.8	30
93	Relation between the Subducting Plate and Seismicity Associated with the Great 1964 Alaska Earthquake. , 1999, , 575-591.		0
94	New seismic images of the Cascadia subduction zone from cruise SO108 — ORWELL. Tectonophysics, 1998, 293, 69-84.	2.2	100
95	Mass and fluid flux during accretion at the Alaskan margin. Bulletin of the Geological Society of America, 1998, 110, 468-482.	3.3	51
96	Crustal structure along the EDGE transect beneath the Kodiak shelf off Alaska derived from OBH seismic refraction data. Geophysical Journal International, 1997, 130, 283-302.	2.4	44
97	The S reflector west of Galicia (Spain): Evidence from prestack depth migration for detachment faulting during continental breakup. Journal of Geophysical Research, 1996, 101, 8075-8091.	3.3	149
98	The case against porosity change: Seismic velocity decrease at the toe of the Oregon accretionary prism. Geology, 1995, 23, 827.	4.4	8
99	Tectonic regime of the southern Kurile Trench as revealed by multichannel seismic lines. Tectonophysics, 1995, 241, 259-277.	2.2	16
100	An automated ray method for diffraction modelling in complex media. Geophysical Journal International, 1994, 116, 23-38.	2.4	10
101	Structure of the Kuril Trench from seismic reflection records. Journal of Geophysical Research, 1994, 99, 24173-24188.	3.3	36
102	Tectonic structure across the accretionary and erosional parts of the Japan Trench margin. Journal of Geophysical Research, 1994, 99, 22349-22361.	3.3	95
103	Wide-angle vibroseis data from the western Rhenish Massif. Tectonophysics, 1990, 173, 83-93.	2.2	6
104	Mass wasting at the base of the south central Chilean continental margin: the Reloca Slide. Advances in Geosciences, 0, 22, 155-167.	12.0	15